OPTIMUM DESIGN OF HEAT EXCHANGER FOR ENVIRONMENTAL CONTROL SYSTEM OF AN AIRCRAFT USING ENTROPY GENERATION MINIMIZATION (EGM) TECHNIQUE

Bello-Ochende T.*, Simasiku E.M. and Baloyi J.†
*Author for correspondence, Department of Mechanical Engineering, University of Cape Town, Rondebosch, 7701,
†Modelling and Digital Science, Council for Scientific and Industrial Research, P.O Box 395, Pretoria, 0001,
South Africa
E-mail: tunde.bello-ochende@uct.ac.za

ABSTRACT

In this paper, the geometrical parameters of two heat exchangers in a typical commercial aircraft's ECS system are designed using the Entropy Generation Minimization (EGM) design technique. The irreversibilities of all the thermodynamic devices in the system are incorporated in the numerical analysis to minimize the exergy destruction of the system. The ECS analysed was based on a bootstrap air cycle with two cooling streams; ram air and air bled from engine fan. The paper proposes optimum air conditions at each device in the system. Trends of varying numerous system parameters against entropy generation number are also investigated to provide the design direction.

INTRODUCTION

Application of the cooling devices in commercial aircraft is subjected to space and weight constraints. The second largest destruction of exergy on an aircraft occurs in the Environmental Control System (ECS) [1]. Due to economic constraints in the industry, current methods employed for thermodynamic optimization of power and cooling devices in aircrafts are inadequate [2]. In account of the aforementioned reasons the EGM technique was used to show that the geometric configuration of compact cross-flow heat exchangers can be deduced by optimizing the global performance of the Environmental Control System (ECS).

The study was based on the bootstrap air cycle ECS consisting of engine components (diffuser, fan and compressor), pre-cooler heat exchanger and an air cycle machine (compressor, ACM heat exchanger and turbine) A comparable air cycle was used by Bejan A et al, and Pérez-Grande et al. in their application of the EGM design tool on aircraft ECS system [3, 4, 1]. However, in most literature the heat exchangers were optimized in isolation from the ECS system. The study optimized the two heat exchangers through integration of all the thermodynamic devices in the system to minimize the exergy destruction of the entire ECS.

ECS focused on employed two cooling streams, the usual ram air and one bled off from the fans to be used in the ACM and the pre-cooler heat exchangers respectively. With fixed external parameters, the entropy generation number of the ECS was written as a function of the free geometrical parameters of the two heat exchangers. This was achieved by using the laws of thermodynamics, heat transfer and fluid mechanics principals.

NOMENCLATURE

C^*	*Capacity ratio*	T	*Temperature* (℃)
b	*Constant,* R/c_p	A	*Total heat transfer area*(m^2)
K_c	*Contraction coefficient*	n_f	*Total number of fins*
A_{fr}	*Core frontal area*(m^2)	V_p	*Volume side plates* (m^3)
V	*Core volume*(m^3)	*Subscripts*	
s	*Entropy* $(J/Kg \cdot K)$	a	*Ambient condition*
N_s	*Entropy generation number*	c	*Compressor*
$\dot{S}_{gen}$	*Entropy generation rate* (W/K)	e	*Conditioning air*
K_e	*Expansion coefficient*	d	*Diffuser*
N_f	*Fin density*$(1/m)$	fan	*Fan*
l	*Fin length*	h	*Hot fluid stream*
t	*Fin thickness(mm)*	i	*Inlet fluid stream*
f	*Flow friction factor*	min	*Minimum*
R_f	*Fouling factor*	n	*Nozzle*
A_o	*Free flow area*(m^2)	opt	*Optimum*
h	*Heat transfer coefficient*$(W/K \cdot m^2)$	o	*Outlet fluid stream*
D_h	*Hydraulic diameter(m)*	w	*Parting wall*
R_{air}	*Ideal Gas constant* (J/kgK)	r	*Ram air*
h'	*Internal fin height(m)*	t	*Turbine*
$L_{x,y,z}$	*Lengths*(m)	*Greek symbols*	
$\dot{m}$	*Mass flow rate*(kg/s)	ρ	*Density* (kg/m^3)
G	*Mass velocity*$(kg/s \cdot m^2)$	τ	*Dimensionless temperature*
N_p	*Number of passages*	$\mu_{h,c}$	*Dynamic viscosity*$(Pa \cdot s)$
Nu	*Nusselt number*	η_f	*Fin efficiency*
U	*Overall heat transfer coefficient*$(W/K \cdot m^2)$	γ	*Fin spacing to height ratio*
Pr	*Prandtl number*	ε	*Heat exchanger effectiveness*
P	*Pressure*(Pa)	η	*Isentropic efficiency*
P	*Pressure(kPa)*	η_o	*Overall surface efficiency*
$\dot{Q}$	*Rate of heat transfer* (W)	σ	*Porosity*
Re	*Reynolds number*	$\mu_{1,2}$	*Ratio of capacity rates*
c_p	*Specific heat capacity* (J/kgK)	β	*Surface area density*(m^2/m^3)
St	*Stanton number*	κ	*Thermal conductivity* $(W/m \cdot K)$

Optimum flow path length was used to set the entropy generation number function of the two heat exchangers was along a minimum path before being integrated into the whole system. Ten programmed numerical methods were used to obtain the minimum entropy generation number of the ECS. Optimization results include the geometrical parameters of the heat exchangers, optimum system air condition configuration and entropy generation number of all the devices in the system. Results obtained from similar studies were used as a base of optimization comparison. Trends were also developed to show the effect of varying the core dimensions of the heat exchangers on the entropy generation number of the entire system, providing some design direction.

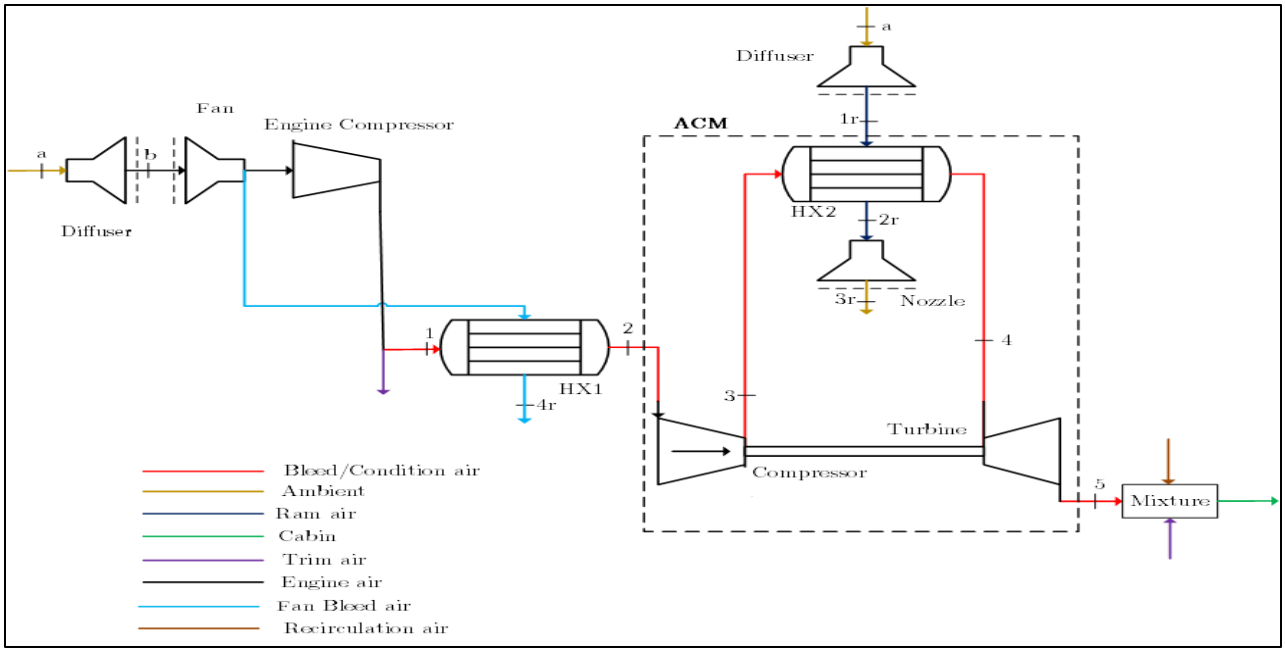

Figure 1 ECS model based on bootstrap air cycle

SYSTEM MODEL DESCRIPTION

Figure 1 shows the concept model of the ECS based on a bootstrap air cycle. Conditioning air enters the system through the engine diffuser; it is then mobilized by the fan into the engine compressor where its temperature and pressure are increased. The air is bled off from the compressor to a pre-cooler heat exchanger where the cold air bled from the fan is used as a coolant. From the pre-cooler, the conditioning air enters the Air Conditioning Machine (ACM) where it passes through a compressor and then an ACM heat exchanger. Bleed air is cooled by Ram air in the ACM heat exchanger. Ram air enters the system through a diffuser and exits through a nozzle. The conditioning air (Bleed air) temperature and pressure are reduced in the turbine before it enters a mixture to be delivered to the cabin and cockpit [3, 1, 4, 5]. The power produced by the turbine is used to drive the compressor.

MATHEMATICAL MODEL

The mathematical model of the system employs a number number of assumptions to help reduce the number of variables and hence the required computational time and power to optimize the system. The assumptions are as follows [3]:

- The ECS operates at steady state. Thus under the assumption of constant density, specific energy and specific entropy of each air stream.
- The air streams were taken to behave like ideal gases with constant specific heat capacity and uniform cross section properties.
- Changes in potential energy are negligible in all devices while kinetic energy changes are only significant in the nozzles and diffusers.
- The analysis is performed for cruise mode of typical commercial jets.
- All devices are adiabatic; heat transfer is only significant in the heat exchangers.
- Duct, pipe and valve losses are negligible

Global Entropy Generation Number

The Gouy-Stodola theorem allows exergy destruction of a system to be reduced by minimizing the entropy generation of the system [6], thus $W_{lost} \sim T_0 S_{gen}$ where T_0 is the environment's absolute temperature. From the second law of thermodynamics, the entropy generation of a system can be written as the sum of the entropy generation of all the thermodynamic devices in the system. As shown in Equation (1)

$$S_{gen} = S_{a-1} + S_{1-2} + S_{2-3} + S_{3-4} + S_{4-5} + S_{a-1r} + S_{2r-3r} \quad (1)$$

In order to effectively use EGM as a design tool, Three dimensionless numbers are introduced, one is the number defined by Bejan in [6] as the entropy generation number (N_s) and the ratio of capacity rates (μ). The numbers are defined as follows:

$$N_s = \frac{S_{gen}}{m_e c_{pe}} \qquad \mu_1 = \frac{m_{fan}\, c_{pa}}{m_e c_{pe}} \qquad \mu_2 = \frac{m_r c_{pa}}{m_e c_{pe}}$$

In accordance with aforementioned dimensionless numbers and the second law of thermodynamics, the entropy generation numbers of the devices under investigation were defined.

ENGINE

The entropy generation number of all the engine components combined was defined as follows:

$$N_{s.engine} = \ln\left(\frac{T_1}{T_a}\right) - b\ln\left(\frac{P_1}{P_a}\right) \quad (2)$$

The engine components considered in this research are the diffuser, fan and the engine compressor. To include the effect of added kinetic energy as the air enters the jet's engine, the stagnation conditions of ambient air were included in the formulation.

The stagnation conditions of air at the engine diffuser were defined as:

$$T_{0a} = T_a\left(1+\frac{\gamma-1}{2}Ma^2\right) \qquad P_{0a} = P_a\left(1+\frac{\gamma-1}{2}Ma^2\right)^{b^{-1}} \tag{3}$$

- **Engine Diffuser**

Stagnation pressure losses in the diffuser are a result of fiction and separation flow regimes [3]. These losses are measured using the isentropic efficiency of the diffuser η_d. The isentropic efficiency is evaluated at stagnation temperature as follows:

$$\eta_d = \frac{V_{bs}^2}{V_{ba}^2} = \frac{h_{bs}-h_a}{h_{ba'}-h_a} = \frac{T_{0bs}-T_a}{T_{0ba'}-T_a} \tag{4}$$

Where T_{0bs} is given by the ideal gas isentropic relation

$$T_{0bs} = T_a\left(\frac{P_{0bs}}{P_a}\right)^b \tag{5}$$

The diffuser was modelled as an adiabatic device, therefore $T_{0b} = T_{0a}$. The diffuser increases the pressure of the air by reducing its velocity; exit pressure at the diffuser is defined by Equation (6)

$$P_{0b} = P_a\left[\eta_d\left(\frac{T_{0a}}{T_a}-1\right)+1\right]^{b^{-1}} \tag{6}$$

- **Engine Fan & Compressor**

Conditions of air at the fan's outlet can be approximated to those at the inlet of the fan. To obtain the stagnation temperature at the exit of the compressor for given bleed pressure, Equation (7) was used assuming equal isentropic efficiency of the compressor and the fan.

$$T_{01} = T_{0b}\left[1+\frac{1}{\eta_c}\left(\left(\frac{P_{01}}{P_{0b}}\right)^b-1\right)\right] \tag{7}$$

At the compressor's outlet, it can be assumed that the Mach number is too low to have any significant influence on the air conditions. Therefore, the static properties can be used. It follows that: $P_{01} \approx P_1$ and $T_{01} \approx T_1$

PRE-COOLER HEAT EXCHANGER

The heat exchangers designed were gas to gas single pass cross-flow compact heat exchanger with offset strips fins. The exergy destroyed in the heat exchanger is due to heat transfer across the fluids and pressure drop in each fluid as it passes through the heat exchanger. The two aforementioned causes of exergy destruction are used to formulate the entropy generation number of the heat exchanger as proposed by Ogulata et al. [7].

- **Offset Strip Fin Properties**

Offset strip fins were chosen for their high goodness factor, as their offset strips enhance heat transfer by periodic interruptions in fluid flow. The fins are also capable of handling a wide range of Reynolds number [8].

Figure 2 above shows the geometrical description of a typical offset strip fin core. As shown in the figure, the geometrical parameters of an offset strip fin surface are described by: (1) Strip length (l); (2) Fin height (h) ; (3) Fin spacing (s); and (4) Fin thickness t. In order to determine the heat transfer and fluid flow data, the dimensionless parameters of the geometry were used. These parameters are; length ratio δ, height ratio α and the spacing ratio γ as defined in Figure 2.

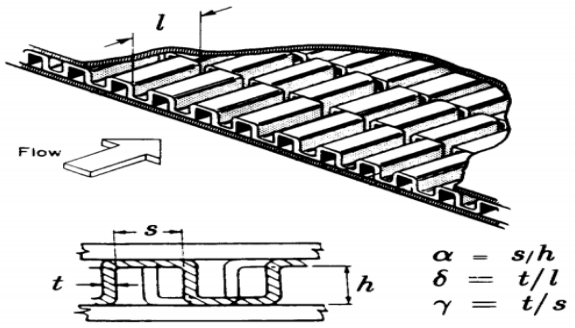

Figure 2 Geometrical description of a typical offset strip fin core [9].

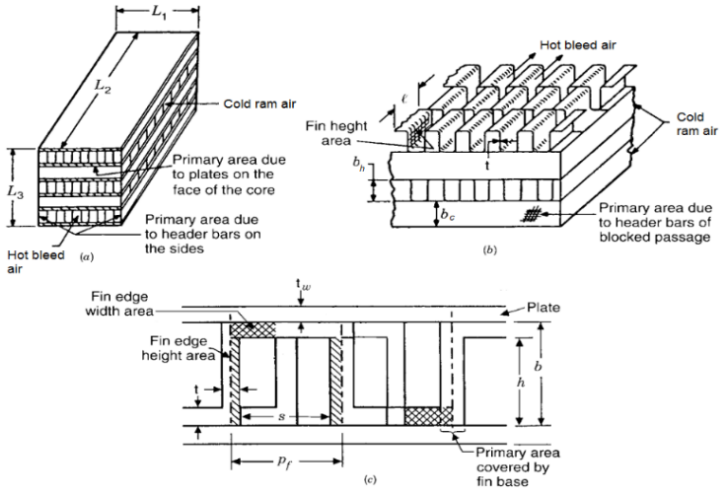

Figure 3 Detailed description of offset strip fin surface geometry characteristic [10]

From Figure 3 two parameters can be defined, the fin pitch ($p_f = s + t$) and plate spacing ($b = h + t$). The figure below shows in detail the geometrical characteristics of an offset strip finned heat exchanger core. The number of passages for both the hot and cold side and the number of fins are required to determine the total heat transfer area. To minimize the heat loss due to temperature difference from ambient conditions, the numbers of passages were assumed to be N_p on the hot fluid side and $N_p + 1$ on the cold fluid side [10]. With the number of passages known the core height was defined as follows.

$$L_z = N_p b_h + (N_p+1)b_c + 2(N_p+1)t_w \tag{8}$$

And the total numbers of fins on each fluid flow stream were defined as follows:

$$n_{f.h} = \frac{L_x}{p_{f.h}}\cdot N_p \qquad n_{f.c} = \frac{L_y}{p_{f.c}}\cdot(N_p+1) \tag{9}$$

Therefore the total primary heat transfer area on each side of the heat exchanger is given by:

$$A_{p.h} = 2L_xL_yN_p - 2t_hL_yn_{f.h} + 2b_hL_yN_p + 2(b_c+2t_w)L_x(N_p+1)$$

$$A_{p.c} = 2L_xL_y(N_p+1) - 2t_cL_xn_{f.c} + 2b_cL_x(N_p+1) + 2(b_c+2t_w)L_yN_p$$

The numbers of offset strip fins on each side of fluid flow passages were defined as follows:

$$n_{off.h} = \frac{L_y}{l_h} \qquad n_{off.c} = \frac{L_x}{lc} \tag{10}$$

The total fin areas on each fluid side were expressed as:

$$A_{f.h} = 2b_h - t_h L_y n_{f.h} + 2b_h - t_h t_h n_{off.h} n_{f.h} + \left(p_{f.h} - t_h\right) t_h \left(n_{off.h} - 1\right) n_{f.h} + 2p_{f.h} t_h n_{f.h}$$
$$A_{f.c} = 2b_c - t_c L_x n_{f.c} + 2b_c - t_c t_c n_{off.c} n_{f.c} + \left(p_{f.c} - t_c\right) t_c \left(n_{off.c} - 1\right) n_{f.c} + 2p_{f.c} t_c n_{f.c} \tag{11}$$

The total heat transfer area is the sum of the total primary area and the total fin area. The total area is expressed as:

$$A = A_p + A_f \tag{12}$$

The total frontal area on the hot fluid side is given by $A_{fr.h} = L_x \cdot L_z$ and $A_{fr.c} = L_y \cdot L_z$ on the cold fluid side. The free-flow area on each fluid side were expressed as $A_{o.h} = (b_h - t_h)(p_{f.h} - t_h)n_{f.h}$ and $A_{o.c} = (b_c - t_c)(p_{f.c} - t_c)n_{f.c}$ respectively. The total inner passage area of the strip over the flow length gives the total surface area of the parting wall $A_w = 2L_x L_y (N_p + 1)$. The volume of the plate on each fluid flow side is given by $V_{p.h} = b_h L_x L_y N_p$ and $V_{p.c} = b_c L_x L_y (N_p + 1)$. The surface area density of the plate on each side was expressed as $\beta = \frac{A}{V_p}$ while the volume of the core is $V = L_x L_y L_z$.

- **Surface Characteristics**

The chosen frictional and heat transfer loss factors for offset strip fins are shown in Equation (13) and Equation (14) as developed by Manglik and Bergles (1995) [9]. The hydraulic diameter of OSF is defined in Equation (15) (Manglik and Bergles, 1990) [11]

$$f = 9.6243\,\mathrm{Re}^{-0.7422}\alpha^{-0.1856}\delta^{0.058}\gamma^{-0.2659} \cdot \left[1 + 7.669\times10^{-8}\,\mathrm{Re}^{4.429}\alpha^{0.92}\delta^{3.767}\gamma^{0.236}\right]^{0.1} \tag{13}$$

$$j = 0.6522\,\mathrm{Re}^{-0.5403}\alpha^{-0.1541}\delta^{0.1499}\gamma^{-0.0678} \cdot \left[1 + 5.269\times10^{-5}\,\mathrm{Re}^{1.34}\alpha^{0.504}\delta^{0.456}\gamma^{-1.055}\right]^{0.1} \tag{14}$$

$$D_{h.MB} = \frac{4 \cdot s \cdot b \cdot l}{2 \cdot s \cdot l + b \cdot l + b \cdot t + s \cdot t} \tag{15}$$

The mass flow velocity of each fluid side of the heat exchanger is given by $G = \dot{m}/A_o$ where A_o is the minimum free-flow area. The mass flow velocity allows the Reynolds's number (Re) to be defined in terms of the hydraulic diameter and material's dynamic viscosity (μ). Reynolds's number, Nusselt number (Nu) and Stanton number (St) were defined as follows.

$$Re = \frac{G \cdot D_h}{\mu} \qquad Nu = \frac{h \cdot l}{\kappa} \qquad St = \frac{Nu}{Re \cdot Pr}$$

- **Heat transfer**

The effectiveness relation of cross-flow compact heat exchangers with both fluids unmixed is shown below.

$$\varepsilon = 1 - \exp\left\{c^{-1} NTU^{0.22} \exp - cNTU^{0.78} - 1\right\} \tag{16}$$

The effectiveness relation allows for the exit temperature of air streams to be determined as follows.

$$T_{h.o} = T_{h.i} - \varepsilon \frac{C_{\min}}{C_h} \cdot \left(T_{h.i} - T_{c.i}\right)$$
$$T_{c.o} = T_{c.i} + \varepsilon \frac{C_{\min}}{Cc} \cdot \left(T_{h.i} - T_{c.i}\right) \tag{17}$$

The dimensionless parameters in the effectiveness relation are the number of transfer units NTU and the heat capacity ratio $c = C^*$. The parameters are expressed as

$$C_h = m_e c_p \qquad C_c = m_{fan} c_p \qquad NTU_1 = \frac{UA}{C_{min1}} \qquad c_1 = \frac{C_{min1}}{C_{max1}}$$

Where $C_{min1}$is the minimum between C_h and C_c while $C_{max1}$is the maximum. The UA term in the NTU expression is defined below.

$$\frac{1}{UA} = \frac{1}{\eta_{o.h} h_h A_h} + \frac{R_{f.h}}{\eta_{o.h} A_h} + \frac{1}{\eta_{o.c} h_c A_c} + \frac{\delta_w}{\kappa_w A_w} + \frac{R_{f.c}}{\eta_{o.c} A_c} \tag{18}$$

The fouling factor of air $R_f = 0.0004 m^2\,K/W$ [12].The heat transfer coefficient (h) on each fluid stream is defined as:

$$h = \frac{j \cdot G \cdot c_p}{\mathrm{Pr}^{\frac{2}{3}}} \tag{19}$$

Defined in terms of the Colburn factor (j), mass flow velocity (G), Prandtl number (Pr) and specific heat capacity (c_p).

In PFHE's the heat transfer surface is extended, hence the heat transfer performance of the surface is measured by extended (or overall) surface efficiency (η_o). The overall efficiency includes the fin efficiency (η_f), which was formulated by assuming adiabatic fin tip with a uniform cross section.

$$\eta_f = \frac{\tanh(m \cdot l)}{m \cdot l} \qquad l = \frac{b}{2} - t \qquad m = \sqrt{\frac{2 \cdot h}{\kappa \cdot t} \cdot \left(1 + \frac{t}{l}\right)}$$
$$\eta_o = 1 - \frac{A_f}{A}(1 - \eta_f)$$

With the above definitions the effectiveness of the heat exchanger can now be written as a function of the free geometric parameters of the heat exchanger

$$\varepsilon_{HX1} = F(L_{x.1}, L_{y.1}, L_{z.1}, N_{f.h}, N_{f.c}, h_h, t_h, h_c, l_c, l_h)$$

Where the core dimensions of the pre-cooler are $L_{x.1}, L_{y.1}, L_{z.1}$

- **Pressure Drop**

The exit pressure along each fluid side are $P_{h1.o} = P_{h1.i} - \Delta P_{h1}$ and $P_{c1.o} = P_{c1.i} - \Delta P_{c1}$. The expressions are evaluated using empirical data for pressure drop in plate-fin heat exchanger [10]. The empirical solution accounts for pressure drop due to three major effects. Entrance effect which is caused by sudden contraction of core inlet, core pressure drop and exist effect caused by sudden expansion at core outlet.

$$\frac{\Delta P}{P_i} = \frac{G^2}{2 g_c \rho_i P_i}\left[1 - \sigma^2 + K_c + 2\left(\frac{\rho_i}{\rho_o} - 1\right) + f\frac{4l}{D_h} \cdot \frac{\rho_i}{\rho_m} - 1 - \sigma^2 + K_e \frac{\rho_i}{\rho_o}\right] \tag{20}$$

The mean density (ρ_m^{-1}) and the porosity (σ) are as defined below.

$$\frac{1}{\rho_m} = \frac{1}{2} \cdot \left(\frac{1}{\rho_i} + \frac{1}{\rho_o}\right) \qquad \sigma = \frac{A_o}{A_{fr}}$$

The Colburn factor j and frictional factor f idealize the fluid properties as being constant. However, experimental data reveal that j and f are temperature dependant. To account for temperature variations in the friction factor, the property ratio method was used since the fluid flow is internal [8]. The method evaluates the properties at bulk mean temperature (T_b) of the outlet temperature of the heat exchanger. The correction requires the wall temperature (T_w) to be defined in order to determine the corrected frictional factor f_2.

$$T_w = \frac{T_{b.h} + \frac{R_h}{R_c} \cdot T_{b.c}}{1 + \frac{R_h}{R_c}} \qquad f_2 = f \cdot \left[\frac{T_w}{T_b}\right]^m$$

The value of exponent (m) depends on the flow region. However for brevity sake the values of laminar flow were used, for heating $m = 1$ and $m = 0.81$ for cooling [13]. For offset strip fins, the contraction (K_c) and expansion (K_e) coefficients are dependent on the Reynolds number, flow cross-sectional geometry, and porosity [10]. Since the flow in offset strip fin is interrupted, the boundary layer does not fully develop. It can be assumed that the flow is fully turbulent with $Re = 10^4$, which is the highest recommended Reynolds number for offset strip fin application [8].

$$K_{c.square} = \frac{1 - 2 \cdot C_{c.tube} + C_{c.tube}^2 \cdot \left(2 \cdot K_{d.square} - 1\right)}{C_{c.tube}^2} \qquad (21)$$

$$K_{e.square} = 1 - 2 \cdot K_{d.square} \cdot \sigma + \sigma^2$$

The jet contraction ratio ($C_{c.tube}$) and velocity-distribution coefficient ($K_{d.square}$) are defined as follows:

$$C_{c.tube} = 4.374 \cdot 10^{-4} \cdot \exp^{6.73\sqrt{\sigma}} + 0.621 \qquad (22)$$

The velocity distribution coefficient for square tube is highly dependent on the Reynolds number apart from the flow cross-section geometry.

$$K_{d.square} = \begin{Bmatrix} 1 + 1.17 \cdot K_{d.tube} - 1 \; if \; Re \geq 2300 \\ 1.39 \qquad otherwise \end{Bmatrix} \qquad (23)$$

Where $K_{d.tube}$ is the velocity distribution coefficient for circular tubes and it is defined as:

$$K_{d.tube} = \begin{Bmatrix} 1.09068 \cdot (4 \cdot f_d) + 0.05884\sqrt{4 \cdot f_d + 1} - 1 \; if \; Re \geq 2300 \\ 1.33 \qquad otherwise \end{Bmatrix}$$

The Reynolds number dependent frictional factor (f_d) is defined as:

$$f_d = \begin{Bmatrix} 0.049 \cdot Re^{-0.2} & if \; Re \geq 2300 \\ \frac{16}{Re} & otherwise \end{Bmatrix} \qquad (24)$$

- **Entropy Generation Number Minimization**

Entropy generation number of the pre-cooler heat exchanger is

$$N_{s.HX1} = \ln\left(\frac{T_2}{T_1}\right) - b\ln\left(\frac{P_2}{P_1}\right) + \mu_1\left[\ln\left(\frac{T_{4r}}{T_b}\right) - b\ln\left(\frac{P_{4r}}{P_{1r}}\right)\right] \qquad (25)$$

This can be re-written as

$$N_{s.HX1} = \ln\left(1 - \varepsilon\frac{C_{\min}}{C_h}\left(\frac{T_1 - T_b}{T_1}\right)\right) - b\ln\left(1 - \frac{\Delta P_{h1}}{P_1}\right) + \mu_1\left[\ln\left(1 - \varepsilon\frac{C_{\min}}{C_c}\left(\frac{T_1 - T_b}{T_b}\right)\right) - b\ln\left(1 - \frac{\Delta P_{c1}}{P_b}\right)\right] \qquad (26)$$

Equation (26) defines the entropy generation number of the pre-cooler as a function of the geometric parameters of the heat exchanger. However, in this research the entropy generation number was first set along a minimum path using optimum flow path length, before being integrated into the whole system.

If the Reynolds number and mass velocity are kept constant, Bejan in [6] argues that the optimum length can be derived such that the entropy generation rate is a minimum. Ogulata et al [7] developed an expression for the optimum flow path length (4L/D) of a cross-flow heat exchanger. The expression is shown in Equation (27).

$$\left(\frac{4L}{D}\right)_{opt} = \left[0.1908 \cdot \frac{\tau^2 c_p}{St^{0.4} \cdot R_{air} \cdot f \cdot G^2}\right]^{\frac{1}{1.4}} \qquad (27)$$

The dimensionless temperature (τ) and dimensionless mass velocity (G^*) are defined below.

$$\tau = \frac{|T_{h.i} - T_{c.i}|}{\sqrt{T_{h.i} T_{c.i}}} \qquad G^* = \frac{G}{\sqrt{2\rho P}}$$

Ogulata et al. [7] expressed the minimum entropy generation number of a cross-flow heat exchanger as

$$N_{s.\min.HX1} = \frac{0.477\tau^2}{\left(\frac{4L}{D}\right)_{opt}^{0.4} \cdot St^{0.4}} \cdot \frac{R_{air}}{c_p} \cdot f \cdot \left(\frac{4L}{D}\right)_{opt} \cdot G^{*2} \qquad (28)$$

According to Bejan [6] minimum entropy generation rates are only compatible with small dimensionless mass velocity, the fluid spends a long time on the heat transfer surface. Therefore the side with the smallest G^* has the highest optimum flow path length; this was considered the limiting case in the evaluation of minimum entropy generation in the heat exchanger. The minimum entropy generation number of the heat exchanger was calculated based on the side with the highest optimum flow path. Evaluation of the Equation [28] leads to the minimum entropy generation number to be defined as a function of the geometric parameters of the heat exchanger

$$N_{s.min.HX1} = F(L_{x.1}, L_{y.1}, L_{z.1}, N_{f.h}, N_{f.c}, h_h, t_h, h_c, l_c, l_h)$$

- **Weight Minimization**

The weight of the heat exchanger can be minimized by reducing the total heat transfer surface area when the parting thickness is kept constant. Heat exchanger mass is given by:

$$M = (A_t + A_c) \cdot t_w \cdot \rho_{Al} \qquad (29)$$

ACM COMPRESSOR

The isentropic temperature and the efficiency of the compressor were calculated as follows:

$$T_{3s} = T_2\left(\frac{P_3}{P_2}\right)^b \qquad \eta_{c.2} \cong \frac{h_{3s} - h_2}{h_{3a} - h_2} = \frac{T_{3s} - T_2}{T_{3a} - T_2}$$

The above definitions allowed for the exit temperature of the compressor to be calculated. A pre-set compression ratio ($\frac{P_3}{P_2}$) of 0.8 was used.

$$T_3 = T_{3a} = T_2 + \frac{T_2}{\eta_{c.2}}\left[\left(\frac{P_3}{P_2}\right)^b - 1\right] \tag{30}$$

The power used by the compressor was determined using Equation (31).

$$W_{comp} = m_e c_p \left\{\frac{T_2}{\eta_{c.2}}\left[\left(\frac{P_3}{P_2}\right)^b - 1\right]\right\} \tag{31}$$

Finally the entropy generation number of the compressor was calculated from the temperatures obtained.

$$N_{s.comp} = \ln\left(\frac{T_3}{T_2}\right) - b\ln\left(\frac{P_3}{P_2}\right) \tag{32}$$

ACM HEAT EXCHANGER

For the ACM heat exchanger, analogous expressions to those defined for the pre-cooler heat exchanger were used. This is due to the fact that the fin arrangements of the two heat exchangers were set to be the same.

The heat capacity rate of the ACM heat exchanger is different from the pre-cooler heat exchanger. They are defined as:

$$C_h = m_e c_p \qquad C_{c.2} = m_r c_p \qquad NTU_2 = \frac{UA}{C_{min2}} \qquad c_2 = \frac{C_{min2}}{C_{max2}}$$

Since the hot side inlet temperature of the ACM heat exchanger depends on the outlet temperature of the pre-cooler, it can be shown that the effectiveness of the ACM heat exchanger is a function of the geometric parameters of the pre-cooler and the ACM heat exchanger.

$$\varepsilon_{HX1} = F(L_{x.1}, L_{y.1}, L_{z.1}, L_{x.2}, L_{y.2}, L_{z.2}, N_{f.h}, N_{f.c}, h_h, t_h, h_c, l_c, l_h)$$

The pressure drop and the entropy generation number can also be expressed as a function of the same variables

$$\frac{\Delta P}{P_i} = F(L_{x.1}, L_{y.1}, L_{z.1}, L_{x.2}, L_{y.2}, L_{z.2}, N_{f.h}, N_{f.c}, h_h, t_h, h_c, l_c, l_h)$$

$$N_{s.min.HX2} = F(L_{x.1}, L_{y.1}, L_{z.1}, L_{x.2}, L_{y.2}, L_{z.2}, N_{f.h}, N_{f.c}, h_h, t_h, h_c, t_c, l_c, l_h)$$

ACM TURBINE

From the ideal gas isentropic relation of turbines, the efficiency of the turbine could be calculated.

$$T_{5s} = T_4\left(\frac{P_5}{P_4}\right)^{-b} \qquad \eta_t \cong \frac{h_4 - h_{5a}}{h_4 - h_{5s}} = \frac{T_4 - T_{5a}}{T_4 - T_{5s}}$$

The outlet temperature at the turbine could now be obtained.

$$T_5 = T_4\left\{1 - \eta_t\left[1 - \left(\frac{P_5}{P_4}\right)^b\right]\right\} \tag{33}$$

The mechanical, hydraulic and thermal losses that the power produced by the turbine has to overcome in order to drive the compressor were taken into account. The power produced by the turbine has to be more than that of compressor ($W_t > W_{comp}$). The power produced by the turbine was defined as:

$$W_t = m_e c_p \eta_t T_4\left(1 - \left(\frac{P_5}{P_4}\right)^b\right) \tag{34}$$

Finally the entropy generation number of the turbine can now be calculated.

$$N_{s.turbine} = \ln\left(\frac{T_5}{T_4}\right) - b\ln\left(\frac{P_5}{P_4}\right) \tag{35}$$

RAM AIR STREAM

- **Diffuser**

Ram air's inlet is at the diffuser. Using the diffuser's inlet diameter A_{di}, the ram air mass flow rate can be obtained from Equation (36) at a given aircraft Mach number

$$m_r = P_a Ma A_{di}\sqrt{\frac{\gamma}{R \cdot T_a}} \tag{36}$$

The Mach number is decreased through the diffuser, only static air properties are considered at the diffuser's outlet. Assuming the adiabatic diffuser $T_{1r} = T_{0a}$, the outlet pressure was obtained from Equation (37).

$$P_{1r} = P_a\left[\eta_d\left(\frac{T_{0a}}{T_a} - 1\right) + 1\right]^{b^{-1}} \tag{37}$$

Therefore the entropy generation number of the diffuser can be obtained:

$$N_{s.diffuser} = \mu_2\left[\ln\left(\frac{T_{1r}}{T_a}\right) - b \cdot \ln\left(\frac{P_{1r}}{P_a}\right)\right] \tag{38}$$

- **Nozzle**

The ram air exits the system through the nozzle to ambient condition. The nozzle exit temperature required to find the entropy generation number of the nozzle is defined by Equation (39), depending on the isentropic efficiency of the nozzle.

$$T_{3r} = T_{2r}\left\{1 - \eta_n\left(1 - \left(\frac{P_a}{P_{2r}}\right)^b\right)\right\} \tag{39}$$

The entropy generation number of the nozzle can be obtained.

$$N_{s.nozzle} = \mu_2\left[\ln\left(\frac{T_{3r}}{T_{2r}}\right) - b \cdot \ln\left(\frac{P_{3r}}{P_r}\right)\right] \tag{40}$$

MINIMIZATION AND SYSTEM CONSTRAINTS

The entropy generation number of the ECS system was expressed as a function of the geometrical and flow parameters of the two heat exchangers. Fixed parameters used in the numerical optimization of the overall system are shown in Table 1below.

The entropy generation number forms a nonlinear system of 14 equations and 14 unknowns:

$$N_{s.min} = F(L_{x.1}, L_{y.1}, L_{z.1}, L_{x.2}, L_{y.2}, L_{z.2}, N_{f.h}, N_{f.c}, h_h, t_h, h_c, t_c, l_c, l_h$$

The systemof equation was solved by using functional iteration in a *Solve Block* in Mathcad 15.0 using the *Minimize* function based on Quasi-Newton. The TOL and CTOL values both set 10^{-3} for precision control.

Table 1 Fixed parameter used in the optimization

Fixed parameters	Unit	Value
Flight conditions		
Ambient temperature(T_a)	$°C$	-60
Ambient pressure(P_a)	kPa	20
Mach number(Ma)		0.85
Altitude(h)	m	12 497
Required Cabin conditions		
Air mass flow rate($\dot{m}_e$)	kg/s	0.804
Cabin temperature(T_{cabin})	$°C$	22
Cabin pressure(P_{cabin})	kPa	75
Adiabatic efficiency		
Diffusers(η_d)		0.97
Engine compressor/fan($\eta_{c.1}$)		0.9
ACM compressor($\eta_{c.2}$)		0.75
ACM turbine(η_t)		0.8
Ram air nozzle(η_n)		0.95
Bleed air pressure(P_1)	kPa	250
Diffuser inlet diameter(A_{di})	m^2	0.012
ACM compression ratio		1.8
Air properties		
Gas constants(R_{air})	$kJ/(kg \cdot K)$	0.287
Specific heat capacity main stream(c_p)	$kJ/(kg \cdot K)$	1.005
Heat capacity ratio(γ)		1.4
Gas constant/heat capacity(b)		0.286
Prandtl Number (Pr)		0.715
Heat exchanger specification		
Parting plate thickness(δ_w)	mm	0.05
Plate conductivity(κ_W)	$W/(m \cdot K)$	190
Fin conductivity(κ_f)	$W/(m \cdot K)$	190
Material density(ρ_{Al})	Kg/m^3	2730
Required condition (Turbine Exit)		
Exit pressure(P_5)	kPa	85

Temperature(K)	**Dynamic viscosity(μ) ($kg/m \cdot s$)**
300	$1.846e^{-5}$
400	$2.286e^{-5}$
500	$2.671e^{-5}$
600	$3.017e^{-5}$

The mass flow rate of air bled off from the fans used in this study was obtained from the C-17A carrier which is $0.1406 kg/s$ [2]

TRENDS AND RESULTS

Table 2 Optimum dimensions for the heat exchangers

Characteristic	**Unit**	**Bleed Air Stream**	**Fan/Ram Air Stream**
Fin height	mm	2.143	1.94
Fin Thickness (t)	mm	0.05	0.305
Fin length (l)	mm	42.795	235.865
Fin Density (N_f)	m^{-1}	445.511	120
Hot Side Length ($L_{x.1}$)	mm	1000	
Cold Side Length ($L_{y.1}$)	mm	42.795	
Height ($L_{z.1}$)	mm	1000	
Hot Side Length ($L_{x.2}$)	mm	1000	
Cold Side Length ($L_{y.2}$)	mm	48.575	
Height ($L_{z.2}$)	mm	1000	

Table 2 summaries the optimum geometry parameters of the heat exchangers for minimum entropy generation in the ECS system as yielded from optimization.

Table 3 Air condition at optimum system configuration

Position	**Temperature (℃)**	**Pressure(kPa)**
a	-60	20
b	-29.2	31.651
1	188.778	250
2	160.186	249.994
3	265.785	449.99
4	127.324	449.986
5	6	85
1r	-29.221	31.651
2r	84.86	26.651
3r	58.089	20

The air conditions (temperature and pressure) values in the system for optimum ECS configuration are summarized in Table 3. The positions in the system refer to ones indicated in Figure 1. The ($6℃, 85\ kPa$) air released from turbine is feed to a mixture where it is mixed with trim air and recirculation air to bring it to required cabin conditions.

Table 4 Final thermal properties for the optimum Pre-cooler Heat exchanger

Parameter	**Unit**	**Hot/Bleed Air Stream**	**Cold/Ram Air Stream**
Outlet Temperature	℃	160.186	134.278
Pressure Drop	Pa	5.583	189.798
Heat Transfer Rate	kW	23.103	
Mass	kg	6.312	
Effectiveness	%	75	
Overall Surface Efficiency		99.8	1
Fin Spacing Ratio		0.023	0.038
Fin Height Ratio		1.024	4.139
Fin Length Ratio		0.001	0.001
$N_{s.min}$		0.074	
Number of Passages		220	221
Total Primary Area	m^2	19.474	3.767
Total Fin Area	m^2	18.009	4.549
Free-flow Area	m^2	0.461	0.018
Frontal Area	m^2	1	0.043
Hydraulic Diameter	m	0.002	0.008
Surface Area Density	m^{-1}	1816.589	319.986

The final optimum thermal and geometry properties of the pre-cooler heat exchanger and ACM heat exchanger are summarized in Table 4 and 5 respectively. At these values the heat exchangers' irreversibilities are at their allowable minimum for least exergy destruction in the ECS. Since the surface area density is greater than $700 m^2/m^3$ and hydraulic diameter is less than 6mm on the hot fluid side in both exchangers, according to [10] the heat exchangers can be classified as compact.

Table 5 Final thermal properties for the optimum ACM Heat exchanger

Parameter	Unit	Hot/Bleed Air Stream	Cold/Ram Air Stream
Outlet Temperature	℃	127.324	84.86
Pressure Drop	Pa	4.16	5000
Heat Transfer Rate	kW	111.879	
Mass	kg	7.422	
Effectiveness	%	46.9	
Overall Surface Efficiency		99.8	1
Fin Spacing Ratio		0.001	0.001
Fin Height Ratio		1.024	4.139
Fin Length Ratio		0.023	0.038
$N_{s.min}$		0.073	
Number of Passages		220s	221
Total Primary Area	m^2	21.965	6.326
Total Fin Area	m^2	20.44	5.146
Free-flow Area	m^2	0.461	0.02
Frontal Area	m^2	1	0.049
Hydraulic Diameter	m	0.002	0.007
Surface Area Density	m^{-1}	1810.552	476.356

The entropy generation numbers of each considered thermodynamic device in the ECS system are summarized in Table 6 below. The values indicate that at optimum configuration, the turbine has the highest entropy generation number meaning it is the most inefficient device in the system. The turbine entropy generation number is influenced by the pre-set conditions of the air bled from the engine compressor. Total is the global minimum entropy generation number of the ECS system.

Table 6 Entropy generation number of all the devices in the system compared with data obtained by Pérez-Grande et al. [3]

Device	Entropy Generation Number	
	Designed System	Pérez-Grande et al.
Engine components	0.052	0.048
Pre-cooler	0.074	9.967×10^{-3}
ACM Compressor	0.05	0.052
ACM Heat Exchanger	0.073	0.017
ACM Turbine	0.115	0.091
Ram air diffuser	0.005	0
Ram air nozzle	0.005	0.801
Total	0.375	1.019

Table 6 above also compares the entropy generation numbers of the devices in the designed system with those obtained from Pérez-Grade et al. [3]. The entropy generation numbers for most of the devices are fairly similar with the exception of the two heat exchangers, turbine and RAM. Pérez-Grande et al. focused mainly on the minimization of the exergy destruction in the two heat exchangers used in the system while this study focused on the overall exergy destruction of the ECS system.

The large difference in Ram air entropy generation number is due to the fact that in the system analysed by Pérez-Grande et al. the Ram air is the only cooling stream used by both exchangers, resulting in a larger temperature difference at the Ram air nozzle. Therefore, the comparison indicates that the designed system is more efficient system in terms of ECS exergy destruction with lower system entropy generation number.

Table 7 Comparison of designed heat exchangers with industry and other studies [1]

		Heat Exchangers			
		Pre-cooler	ACM	Industry	Vargas et al.
Compact plate-fin single pass cross-flow with both fluids unmixed					
Fin Geometry		Offset Strip Fin		Finless	Plain Fin
Hot Side Length	m	1		0.546	0.207
Cold Side Length	mm	42.8	48.6	106	334
Height	m	1		0.738	0.620
Plate Separation(hot)	mm	2.193		1.9	1.6
Plate Separation(cold)	mm	2.245		3.2	3.3
Plate Thickness	mm	0.05		0.15	0.15
Material		Al 3003		Steel	Steel
Overall Mass	kg	6.312	7.422	19.4	20
Entropy Generation Number		0.074	0.073	0.217	0.058

A comparison of the designed heat exchangers with one used in industry and one designed by Vargas et al. [1] is shown in Table 7 above. The designed heat exchangers are optimum in terms of weight with respects to the other heat exchangers. The weight difference is a result of Aluminium used instead of the steel employed by the counter parts. The entropy generation numbers of the two designed heat exchanger is much lower than that of the one used in industry and fairly close to one obtained by Vargas et al. using a comparable design approach.

- ***Simulation Results***

To investigate the effect of heat exchangers' core dimensions on the entropy generation number of the system, the geometrical parameters of the heat exchangers were fixed to develop numerous trends. The fixed values used are shown in Table 8 below.

Table 8 Fixed values used in the simulation

		Pre-cooler HX	ACM HX
Core Volume	m^3	0.5	0.5
Fin thickness	mm	0.05	0.305
Fin Height	mm	2.143	1.94
Fin Length	mm	42.795	235.865
Fin Density	m^{-1}	445.511	120

Figure 4 below depicts the variation of the heat transfer and pressure drop on the overall entropy generation number of the ECS. As the entropy generation number increases, the figure shows that the heat transferred in the heat exchangers remains relatively the same with only a slight increase.

The results were expected as the trend was plotted at the optimum heat transfer surface, which suggest that the optimum heat transfer surfaces are robust at various core dimensions. The pressure drop at cold fluid side is much higher in both heat exchangers; this is due to higher mass velocity of the fluid as a

result of smaller free flow area. The graph shows that an increase in pressure drop will result in an increase in entropy generation number.

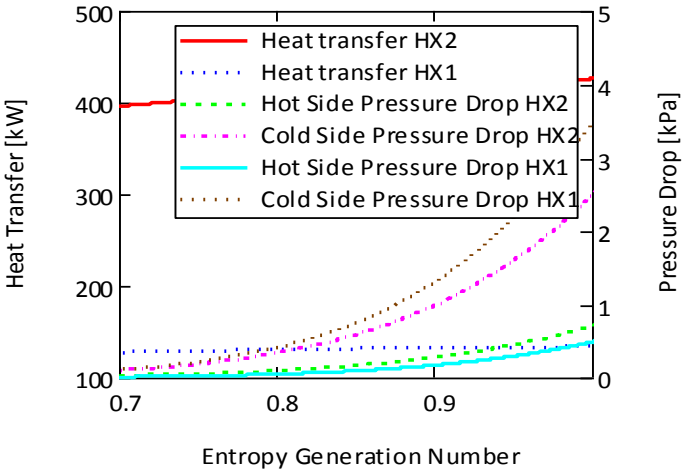

Figure 4 Effect of heat transfer and pressure drop on entropy generation number

Figure 5 and Figure 6 show the variation between core dimensions of the heat exchangers and ECS minimum entropy generation number with the effectiveness of the respective heat exchangers. Both graphs indicate that as the effectiveness of heat exchangers increase, as the flow lengths of heat exchangers and the entropy generation number increase but the non-flow lengths decreases. This proposes that in order to obtain a lower entropy generation number, one must be willing to compromise on the effectiveness and track the height of the heat exchanger to ensure that it is within acceptable limits.

Figures 7, investigate the effect of heat exchanger size on the entropy generation number. For a given overall heat coefficient and minimum heat capacity rate, NTU is the measure of the overall heat surface area of the heat exchanger. Therefore large heat exchangers can be characterized as having large NTU. Figure 7 depicts that smaller heat exchangers are required to minimize the ECS entropy generation number of the ECS.

CONCLUSION

The results indicates that it is possible deduce complete geometric structure of heat exchangers by using EGM technique while accounting for entropy generation rates of all the thermodynamic devices in the system. In addition, the optimization criteria of minimizing the weight and entropy generation could be simultaneously met. Trends indicate that smaller heat exchangers should be employed in the ECS to minimize the destroyed exergy in the system.

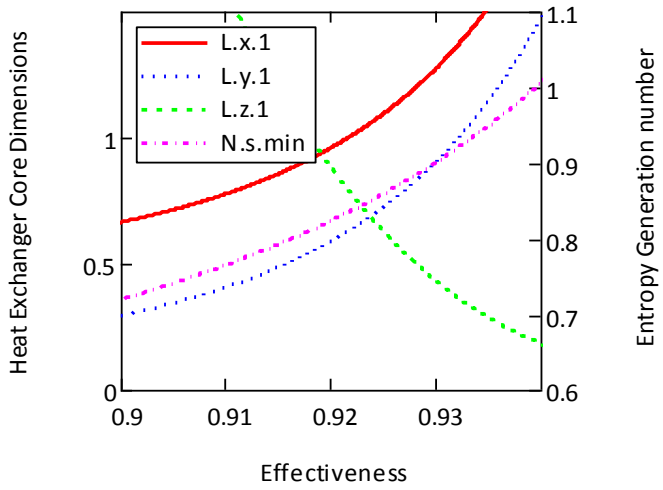

Figure 5 Effect of core dimensions and entropy generation number on the effectiveness of the pre-cooler heat exchanger

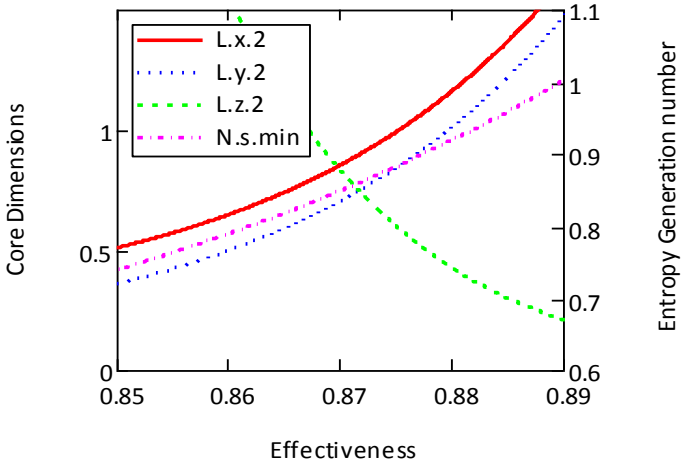

Figure 6 Effect of core dimensions and entropy generation number on the effectiveness of the pre-cooler heat exchanger

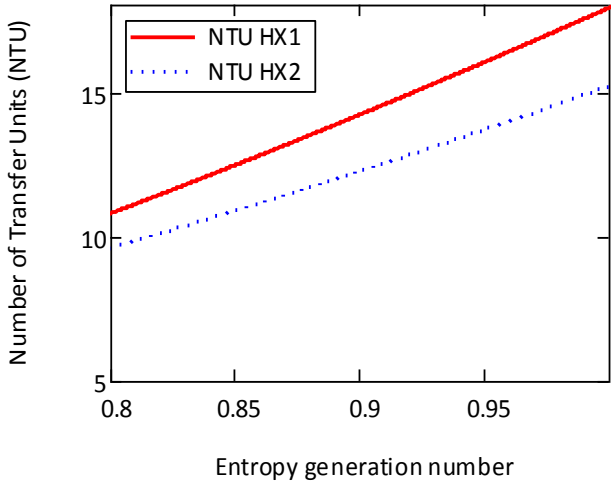

Figure 7 Effect of heat exchanger size on entropy generation number

REFERENCES

[1] J. V. Vargas and A. Bejan, "Integrative thermodynamic optimization of the environmental control system of an aircraft," *International journal of Heat and Mass Transfer*, vol. 44, no. 20, pp. 3907-3917, 2001.

[2] A. Bejan and D. L. Siems, "The need for exergy analysis and thermodynamic optimization in aircraft development," *Exergy, An International Journal*, vol. 1, no. 1, pp. 14-24, 2001.

[3] I. Pérez-Grade and T. J. Leo, "Optimization of a commercial aircraft environmental control system," *Applied Thermal engineering*, vol. 22, no. 17, pp. 1885-1904, 2002.

[4] J. V. Vargas and A. Bejan, "Thermodynamic optimization of finned crossflow heat exchangers for aircraft environmental control system," *International Journal of Heat and Fluid Flow*, vol. 22, no. 6, pp. 657-665, 2001.

[5] I. Martinez, "Aircraft Environmental Control," 1995 - 2015.

[6] A. Bejan, Entropy Generation Minimization The Method of Thermodynamic Optimization of Finite-Size Systems and Finite-Time Processes, United States of America: CRC Press LLC, 1996.

[7] R. T. Ogulata and F. Doba, "Experiments and entropy generation minimization analysis of a cross-flow heat exchanger," *heat Transfer Engineering*, vol. 41, no. 2, pp. 373-381, 1998.

[8] K. Thulukkanam, Heat Exchanger Design Handbook, New York: CRC Press, 2013.

[9] R. M. Manglik and A. E. Bergles, "Heat Transfer and Pressure Drop Correlations for the Rectangular Offset Strip Fin Compact Heat Exchanger," *Experiemental Thermal and Fluid Science*, vol. 10, pp. 171-180, 1995.

[10] R. K. Shah and D. P. Sekulic, Fundamentals of heat exchanger design, New jersey: John Wiley & Sons, 2003.

[11] H. M. Teruel, Y. C. Nakashina and P. Paglione, "Rectangular Offset Strip-fin Heat Exchanger Lumped Parameter dynamic model," *Brazilian Symposium of Aerospace Eng. & Application*, 2009.

[12] Y. A. Çengel and A. J. Ghajar, Heat and Mass Transfer, Singapore: McGraw-Hill Education, 2015.

[13] H. M. Joshi and R. L. Webb, "Heat transfer and friction in the offset strip-fin heat exchanger," *International Journal of Heat and Mass Transfer*, vol. 30, pp. 69-84, 1987.